NAPHTHYL- *VS*. ANTHRYLPYRIDINE-2,6-DICARBOXAMIDES IN CATION BINDING STUDIES. SYNTHESIS AND SPECTROSCOPIC PROPERTIES

Natalia Łukasik[a], Ewa Wagner-Wysiecka[a], Véronique Hubscher-Bruder[b], Sylvia Michel[b], Maria Bocheńska[a] and Beata Kamińska[a]

[a]Faculty of Chemistry, Department of Chemistry and Technology of Functional Materials, Gdansk University of Technology, Gdansk, Poland; [b]Université de Strasbourg, IPHC, CNRS, UMR7178, Strasbourg, France

Contact: Ewa Wagner-Wysiecka, ewa.wagner-wysiecka@pg.gda.pl

Abstract: Pyridine-2,6-carboxamides bearing α- or β-naphtyl- and α- or β-anthryl residues were prepared using simple method from pyridine-2,6-carboxylic acid dichloride and the respective aromatic amines. For the obtained receptors, selective binding of lead(II) and copper(II) was found. Ion-receptor interactions were studied using UV-vis spectroscopy, spectrofluorimetry, ^{1}H NMR and FTIR spectroscopy. The reversible lead(II) and copper(II) binding was discussed in regard of type of aromatic residue and amide bond localization in aromatic ring, and binding model was proposed.

Keywords: pyridine-2,6-dicarboxamides; naphthylamide; anthrylamide; ion molecular recognition; spectroscopic methods

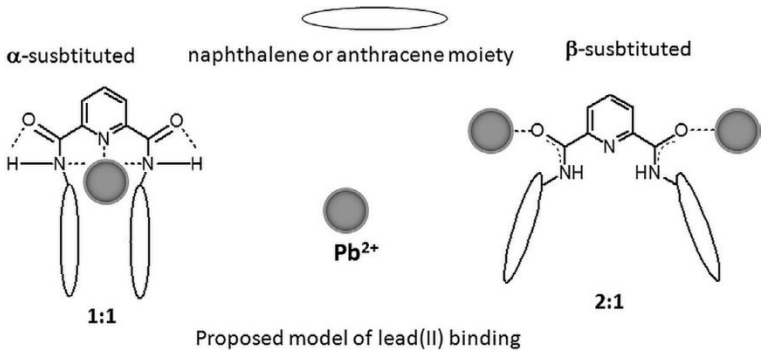

Proposed model of lead(II) binding

1. Introduction

Molecular ion receptors gained many interest during the last decades due to high importance of metal cations and anions complexation in many fields, e.g. biochemistry, environmental protection, industrial processes and many others (*1*). Ions, essential macro- and microelements, are ubiquitous in nature; however, their excess can be dangerous for human health and environment. For instance, the presence of Pb^{2+} in human body leads to immune, nervous and cardiovascular system disorders (*2, 3*). Copper, an element which plays an important role in biological systems (e.g. tyrosinase, ferroxidases, dopamine beta hydroxylase), is harmful to the cells: as a free ion causes blood haemolysis, as well as liver and kidney damage (*3*). Therefore, molecular receptors allowing quick and selective ion recognition are still highly demanded. Compounds bearing chromogenic and/or fluorogenic moieties can serve as convenient analytical tools, where information about molecular recognition is transformed into colour and/or fluorescence change also enabling naked-eye ion sensing (*4*). For instance, chromogenic and fluorescent naphthalene or anthracene derivatives proved to be an effective signal recognition element for metal cations (*5*), halides (*6*) or oxyanions (*7*). Aromatic rings can also play a key role both in reversible ion binding and perfectly organised supramolecular self-assembly systems (*8*).

An interesting group of ion receptors seems to be pyridine-2,6-dicarboxamides forming stable complexes with metal cations (*9*). For example, *N,N,N′,N′*-tetra-ethylpyridine-2,6-dicarboxamide reported by Renaud and co-workers (*10*) forms stable complexes with trivalent

lanthanide ions. Picot et al. (*11*) described a series of chromogenic pyridine-2,6-dicarboxamides showing affinity to Eu^{3+} in acetonitrile. Complexes of pyridine-2,6-dicarboxamides with Ni^{2+} were used in CO_2 conversion to bicarbonate or carbonate (*12*), while chromium(III) and manganese(III) complexes were proposed as inexpensive catalysts for alkene epoxidation and alkane hydroxylation (*13*).

Pyridine-2,6-carboxamides exhibit antibacterial, antifungal, antitubercular properties (*14*) and some of them were investigated as anticancer drugs (*15*). Metal complexes of 2,6-pyridine dicarboxylic acid were found to have beneficial effect in normalising elevated blood glucose levels in rats (*16*). It was also demonstrated that copper(II) complexes of *N*-2-(2-pyridylmethyl)-2-pyridinecarboxamide behave as inhibitors of HIV-1 PR (*17*).

Above facts allow us to conclude that ion recognition mechanism can be important in the design and synthesis of new compounds bearing pyridine-2,6-dicarboxamide moiety, especially bioactive substances based on amide structure.

Here, we describe synthesis and ion binding properties of pyridine-2,6-dicarboxamides bearing naphthyl or anthryl residues (Scheme 1). Ligand **1** was synthesised before by Hiratani and co-workers (*18*). Ghosh et al. showed its ability to Ru^{2+} coordination in solution and in a solid state (*19*). A crystal structure of **2** was reported by Qi (*20*). Ligands **3** and **4**, to the best of our knowledge, have not been described in the literature so far (according to Chemical Abstracts). The introduction of condensed aromatic rings makes the mentioned receptors active in UV–vis region enabling molecular recognition studies with simple and easily accessible instrumentation. As amide bond can act as metal cation binding site (*21*), spectroscopic response towards metal cations is discussed in terms of type of aromatic residue and location of amide bond in an aromatic ring. The ion binding mechanism was proposed on the basis of proton nuclear magnetic resonance and infrared spectroscopies.

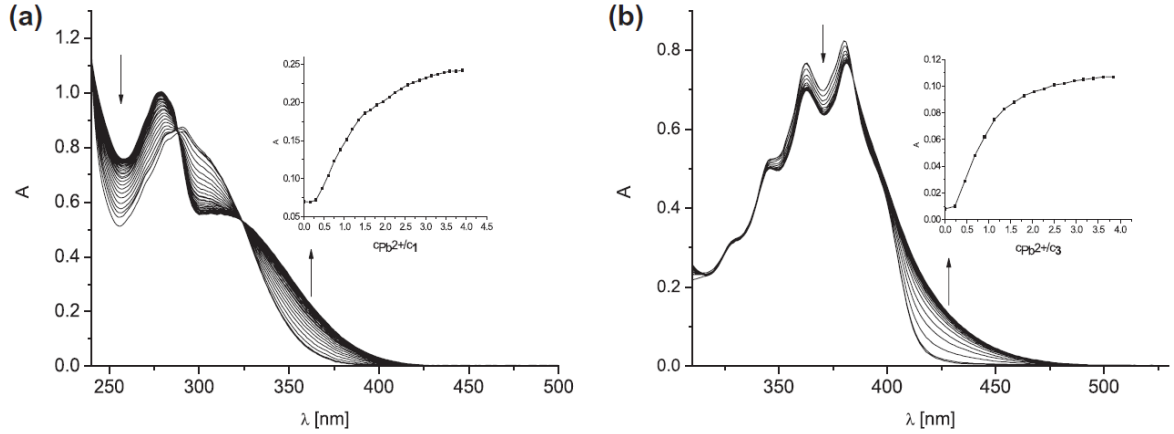

Figure 1. Changes in the UV-vis spectra upon titration with $Pb(ClO_4)_2$ (a) ligand **1** (c_L = 5.02 × 10^{-5} M, 0 ≤ R ≤ 3.63) and (b) ligand **3** (c_L = 6.01 × 10^{-5} M, 0 ≤ R ≤ 3.27) in acetonitrile. Insets show the respective molar ratio plots. R: salt/ligand molar ratio.

2. Results and discussion

2.1. Synthesis

The synthetic route for ligands **1**–**4** is presented in Scheme 1. Amides **1**–**4** were prepared according to the synthetic procedures described by us previously (*22, 23*). Pyridine-2,6-carboxylic acid dichloride was added in portions to a solution of the respective aromatic amine in dry dimethylformamide (DMF). Triethylamine was used as an HCl scavenger. Reaction was carried out at 60°C for 12 h. Amide **1** was obtained previously by Hiratani et al. (*18*) in only slightly higher yield (81%) than in reaction presented here, i.e. 77%, where DMF instead of carcinogenic benzene was used as a solvent. Ghosh and co-workers (*19*) obtained compound **1** using DCC method with 55% yield.

Crystal structure of amide **2** was reported by Qi et al. (*20*); however, neither reaction yield nor spectral characteristics for it was given. We obtained compound **2** with a satisfactory yield of 70% and its complete spectral characterisation is given in Experimental Section. New ligands **3** and **4** – aminoanthracene derivatives – were obtained with lower than their naphthyl analogues yields. Especially, compound **3** for which rather moderate yield of 26% is reported here. Even so, proposed here procedure seems to be a facile method for amide preparation.

2.2. Ion complexation studies

Although ligands **1** and **2** are known (*19, 20*), their ion binding ability has not been investigated exhaustively so far. In our previous work, we have signalised ion binding properties of **2** (*24*). Here, we present more detailed metal cation recognition studies for compounds **1** and **2** and new amides **3** and **4**. Currently, ability of ligands to anionic species binding is also being examined, what will be published elsewhere.

2.2.1. Metal cation complexation

Alkali (Li^+, Na^+, K^+), alkaline earth (Mg^{2+}, Ca^{2+}, Sr^{2+}, Ba^{2+}) and heavy divalent metal cations (Co^{2+}, Ni^{2+}, Zn^{2+}, Cu^{2+}, Pb^{2+}) binding was studied in aprotic solvents by spectroscopic methods (UV–vis, ^{1}H NMR spectroscopy). In highly dipolar DMSO, metal cations caused no significant spectral changes. In less polar acetonitrile, selective response of compounds **1**–**4** towards lead(II) and copper(II) perchlorates was observed.

Spectrophotometric titrations with lead(II) perchlorate in acetonitrile revealed that ligands **1** and **3**, bearing *α*-substituted aromatic rings, interact with this cation in a similar way. According to the molar ratio plot and titration data, it can be concluded that, for both ligands, the equilibrium is reached at equimolar amount of ligand and salt. Additionally, well-defined isosbestic points suggest 1:1 complex formation under titration conditions. Changes upon spectrophotometric titration of ligands **1** and **3** with lead(II) perchlorate in acetonitrile and the respective molar ratio plots are shown in Figure 1.

The interpretation of the spectrophotometric data shows the formation of PbL species of comparable, but slightly higher for ligand **3**, stability for both ligands (Table 1). These results reveal the same behaviour of both ligands **1** and **3** towards Pb^{2+}.

Table 1. Stoichiometries (Pb:L) and values of stability constants (log ***β***) for Pb^{2+} complexes with ligands **1-4** in acetonitrile.

Pb:L aromatic ring substitution	Ligand **1 α-**	Ligand **2 β-**	Ligand **3 α-**	Ligand **4 β-**
1:1	4.30±0.11	-	4.46±0.06	-
2:1	-	9.02±0.05	-	9.40±0.22

Ligands **2** and **4** containing *β*-substituted aromatic rings interact with Pb^{2+} differently than their α-substituted analogues. Spectral changes upon spectrophotometric titration of **2** and **4** with lead(II) perchlorate in acetonitrile are shown in Figure 2. Considering the fit for different models, for both ligands, the most probable binding model is 2:1 (Pb:L).

The reversible complexation/decomplexation of lead(II) was possible to trigger by changing the pH (TBAOH) of solution. From UV–vis measurements, the detection limits (L_D) of amides **1**–**4** for lead cation were found to be respectively for **1**/**2**/**3** and **4**: 4.62×10^{-6}/1.08×10^{-5}/1.39×10^{-6} and 8.41×10^{-7} M.

The spectrophotometric results obtained for ligands **1**–**4** show that stoichiometry of Pb^{2+} complexes depends on the position of aromatic ring substitution. Amides derived from *α*-substituted amines (compounds **1** and **3**) form 1:1 complexes in acetonitrile, whereas 2:1 (Pb:L) complexes appear to be dominant for amides with *β*-substituted aromatic ring.

This is probably related to spacial structure of amides and a possibility of forming a more rigid molecular pseudo-cavity by *α*-substituted derivatives. *β*-Substituted condensed aromatic ring, especially anthracene, and carbonyl group can accommodate more flexible

geometry (*25*). The type of aromatic residue also influences the strength of Pb^{2+} binding n acetonitrile. Anthracene derivatives, regardless of the stoichiometry of complexes, bind Pb^{2+} slightly stronger than amides with naphthalene moiety.

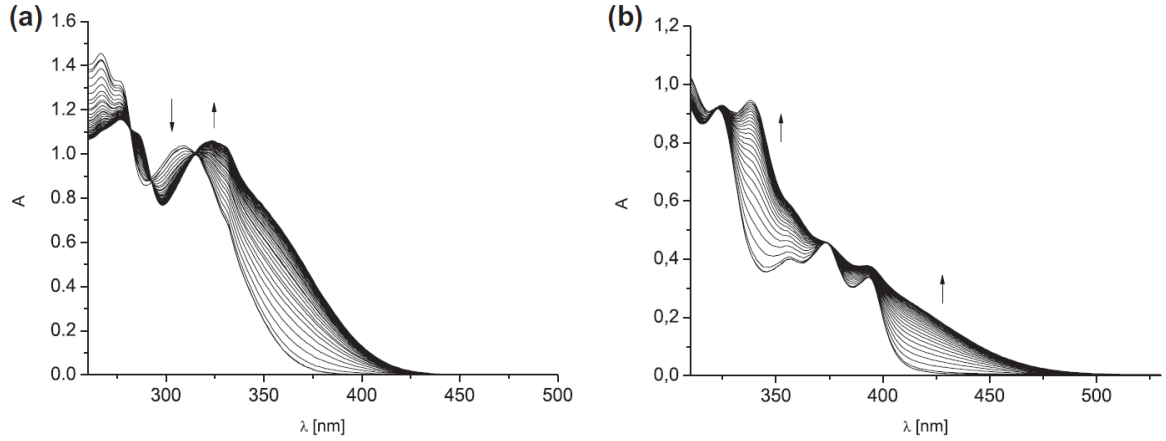

Figure 2. Changes in the UV-vis spectra upon titration of the ligand with $Pb(ClO_4)_2$ (a) **2** (c_L = 2.50 × 10^{-5} M, 0 ≤ R ≤ 2.00) and (b) **4** (c_L = 3.27 × 10^{-5} M, 0 ≤ R ≤ 5.55) in acetonitrile. R: salt/ligand molar ratio.

Secondary amides can strongly bind transition metal cations via deprotonated N-amide atom or in their neutral form (*21*). Coordination of metal ion can also occur with an engagement of O-amide atom. A similar situation can be considered for heavy lead(II) cation. For better understanding of lead(II) complexation, ^{1}H NMR spectra for ligands **3** and **4** were registered in the presence of lead(II) perchlorate in acetone-d_6.

In spectrum of **3**-**Pb** complex (Figure 3), N–H amide proton signal shifts from 11.16 ('free' ligand) to 11.51 ppm ($\Delta\delta$ = +0.35 ppm) in lead(II) complex. It points the formation of stronger than in 'free' ligand hydrogen bond. In the spectrum of complex, all signals of anthracene protons show well-defined multiplets and higher shielded protons comparing to 'free' ligand. It suggests that lead(II) complexation is a driving force for ligand preorganization and probable participation of these fragments of the molecule in complex formation. Additionally, shielding ($\Delta\delta$ = +0.50 ppm) of A-labelled pyridine proton in *para* position to nitrogen atom (seen as triplet at 8.49 ppm in 'free' ligand spectrum) and B-labelled protons points engagement of pyridine nitrogen atom in lead(II) complexation. This is in agreement with crystallographic data reported for metal complexes of ligands of similar stucture (*26*), where metal cation is bound via two nitrogens of amide moiety and nitrogen atom of pyridine skeleton. FTIR spectroscopy can provide additional information of metal cation binding sites in amide derivatives (*27*). Analysis of FTIR spectrum (KBr pellet) of **3** and the same sample for which ^{1}H NMR spectrum was registered (Figure 4(a) and (b)) shows changes in the *v*(N–H) band. Relatively broad, hardly splitted bands at 3385 and 3371 in 'free' **3** appear as one sharp peak at 3385 cm^{-1} for lead(II) complex suggesting formation of stronger hydrogen bond upon metal cation complexation. Amide I *v*(C=O) band shifts from 1687 to 1690 cm^{-1}. The amide II band in 'free' ligand is observed as splitted signal at 1548 and 1530 cm^{-1} suggesting different involvment of N–H residues in hydrogen bond formation. In complex, it appears as single, sharp peak at 1524 cm^{-1} pointing changes in ligand symmetry upon lead(II) complexation. Spectral data for ligand **3** let us conclude that lead(II) is bound by neutral ligand through the nitrogen amide and pyridine moiety atoms.

Analogous experiments were carried out for ligand **4**. In ^{1}H NMR spectrum of **4** (Figure 5) recorded in the presence of Pb^{2+}, less shielding of amide N–H proton ($\Delta\delta$ = +0.20 ppm) suggests the formation of weaker, comparing to **3**, hydrogen bonds upon metal cation complexation. The most noticable changes in aromatic proton shifts are observed for anthracene protons labelled as K ($\Delta\delta$ = +0.10 ppm) and pyridine skeleton proton signals

labelled as A and B (~$\Delta\delta$ = +0.38 and + 0.22). For remaining aromatic signals, shifts are less spectacular.

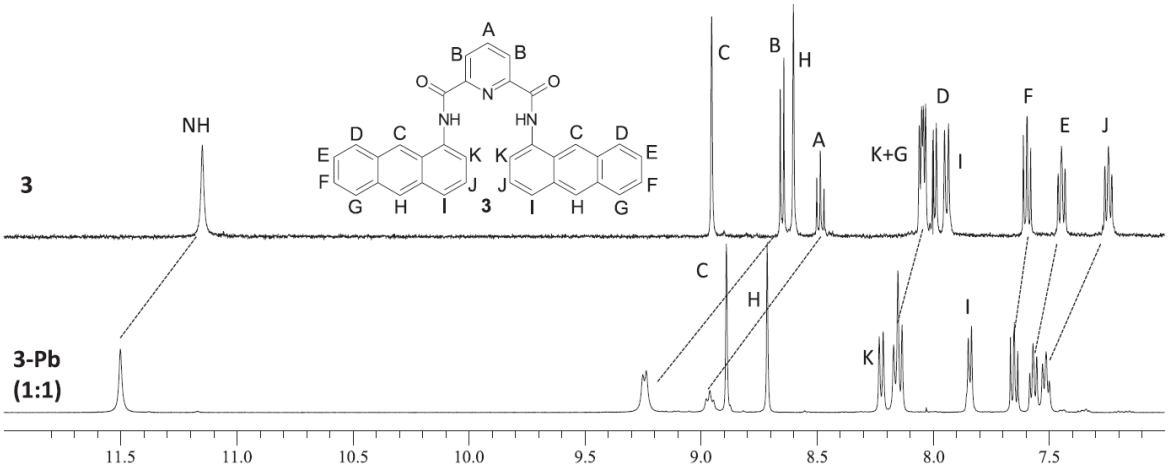

Figure 3. Differences in ^{1}H NMR spectra of **3** and **3-Pb** complex in acetone-d_6.

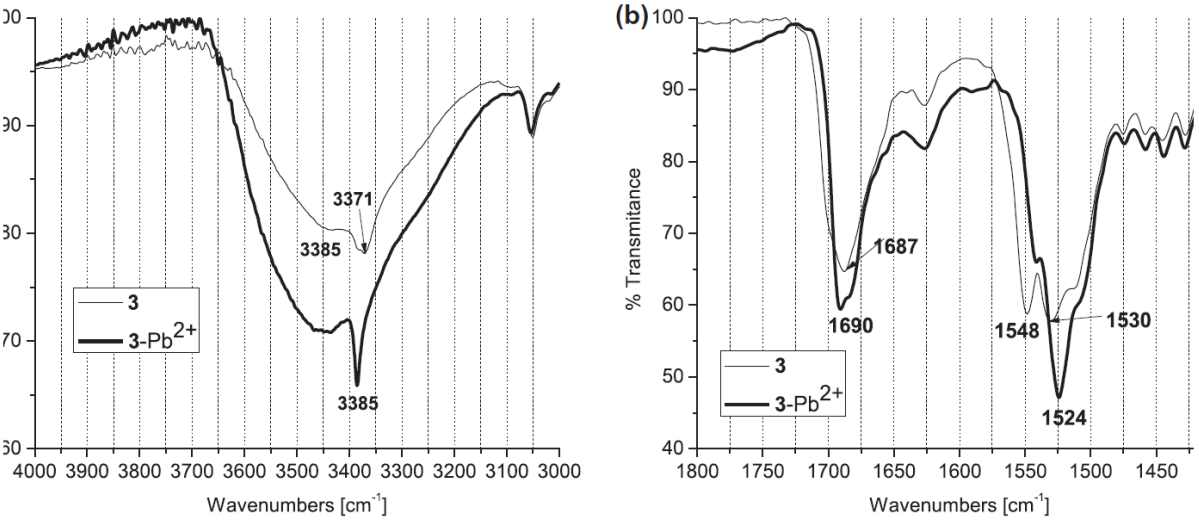

Figure 4. (a), (b) Comparison of normalised FTIR spectra (KBr pellet) of ligand **3** and its complex with lead(II) perchlorate (excess of salt).

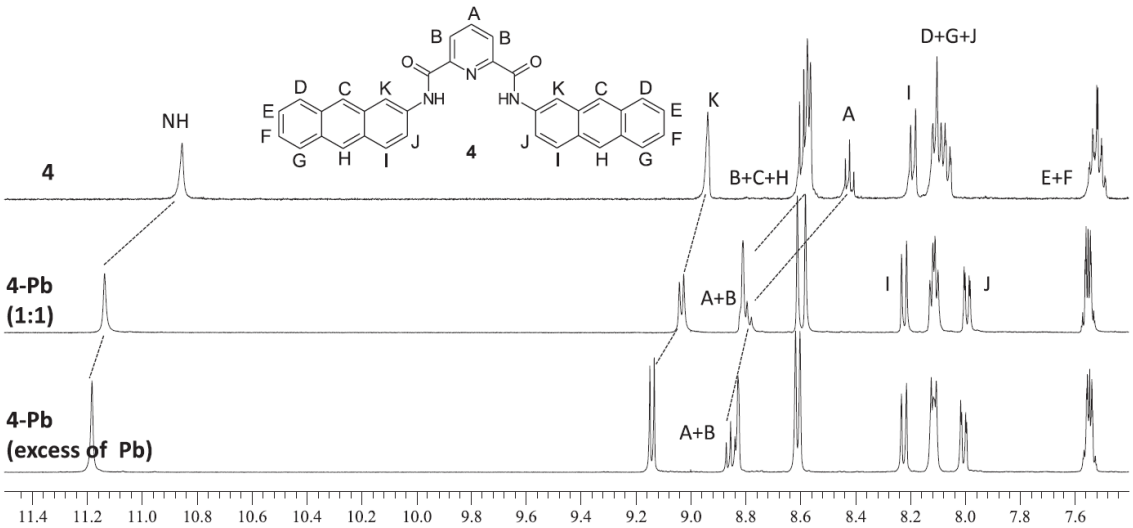

Figure 5. Differences in ^{1}H NMR spectra of **4** and **4-Pb** complex in acetone-d_6.

In FTIR spectrum (Figure 6) of **4**–Pb complex, the amide I band is shifted to lower and the amide II bands to higher frequency. It points out the decrease of double bond character of C=O and the increase of C–N double bond character as a consquence of Pb^{2+} binding through oxygen amide atoms.

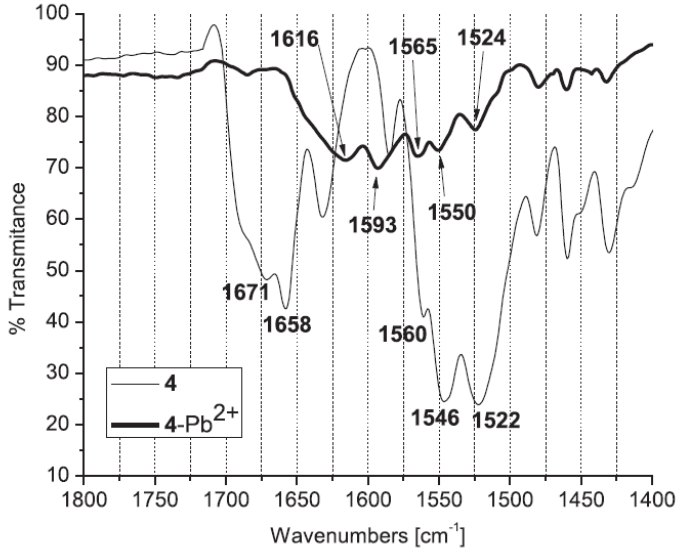

Figure 6. Comparison of normalised FTIR spectra (KBr pellet) of ligand **4** and its complex with lead(II) perchlorate (excess of salt).

Differences in Pb^{2+} complexation for ligands **3** and **4** can be connected with the place of anthracene ring substitution affecting the geometry of free ligands. The optimised model of 'free' ligand **3** showing its pseudo-cavity as a distance (Å) between labelled amide nitrogens and C–C aromatic atoms and its comparison with 'free' **4** model are shown in Figure 7.

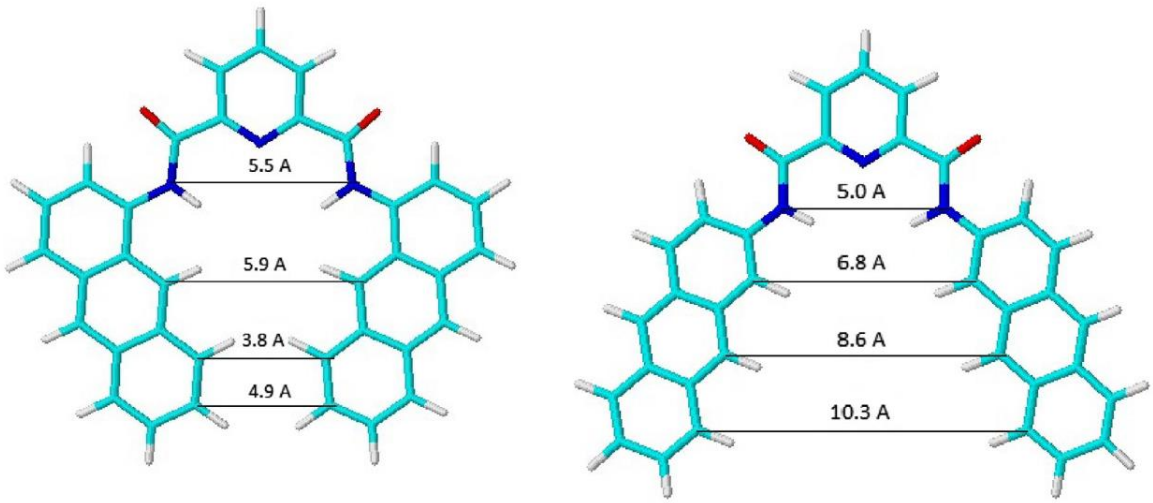

Figure 7. Optimised structures (AM1) of 'free' ligands **3** and **4** showing size of molecular pseudo-cavity as a distance of N–N and C–C atoms.

In proposed models of **3** and **4**, the conformation of amide group where N–H atoms are directed towards the centre of the pseudo-cavity is in agreement with the data reported for 2,6-dicarboxamides (*23, 28*).

On the basis of results presented above, we propose a Pb^{2+} binding mechanism for ligands **3** and **4** as shown in Figure 8.

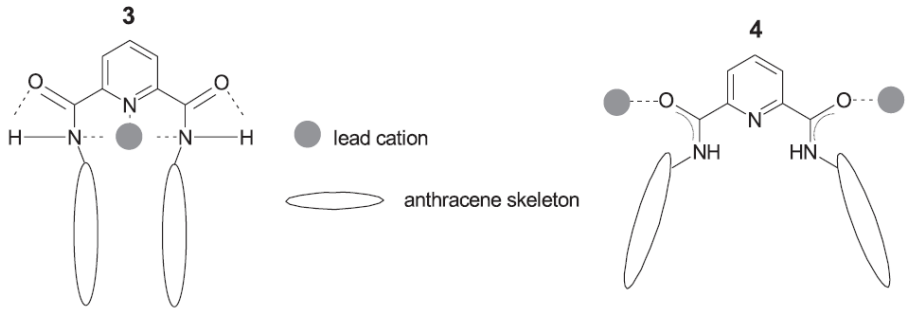

Figure 8. Proposed model for lead(II) binding by ligands **3** and **4**.

Concluding, it can be stated that the more rigid anthracene in **3** is crucial for lead(II) effective binding via amide nitrogen atoms in 1:1 complex. Ligand **4**, also in neutral form, creates complexes in which two lead(II) cations are coordinated through oxygen amide atoms.

Fluorescence measurements carried out in acetonitrile for ligands **3** and **4** showed that the presence of lead(II) perchlorate causes fluorescence quenching (Figure 9).

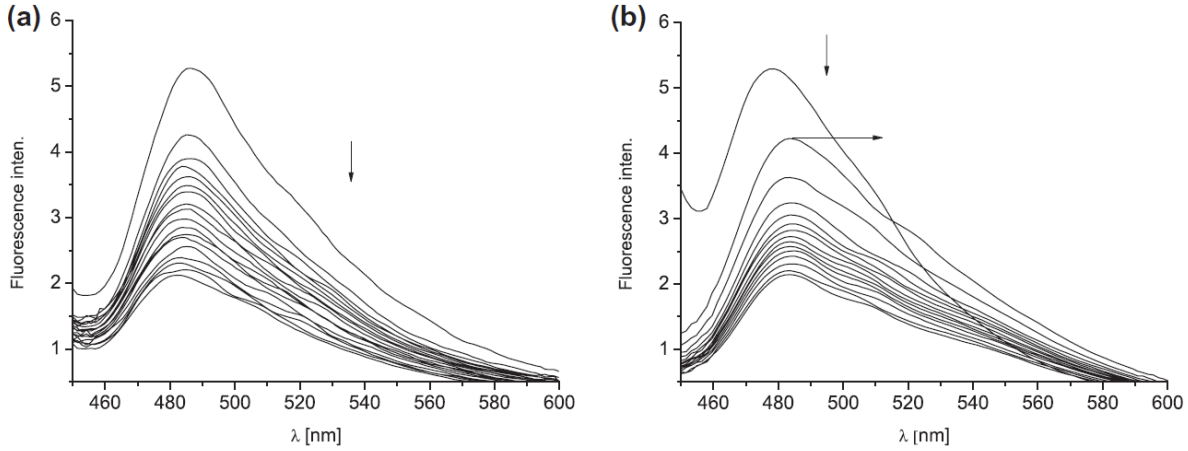

Figure 9. Changes in fluorescence spectra of ligands upon titration with $Pb(ClO_4)_2$ (a) **3** (c_L = 3.29 × 10^{-5} M, 0 ≤ R ≤ 17.70, λ_{ex} = 340 nm, λ_{em} = 490 nm) and (b) **4** (c_L = 4.44 × 10^{-5} M, 0 ≤ R ≤ 12.50, λ_{ex} = 340 nm, λ_{em} = 490 nm) in acetonitrile. R: salt/ligand molar ratio.

Under fluorescence measurement conditions, molar ratio plots point the formation of 1:1 and 2:1 Pb^{2+} complexes with ligands **3** and **4**, respectively (Figure SM1a and b, Supplementary Data). These results are in agreement with UV–vis results. Stern–Volmer plots (*29*) (Figure SM2, Supplementary Data) for both sytems including the respective ligand and lead(II) perchlorate are similar: downcurved with linear dependence only in the range of low concentrations of quencher. At this point, it can only be assumed that under the measurment conditions, fluorescence quenching is probably caused by both collisional and static quenching. Nonlinearity of the data for **4** can also be due to the formation of 2:1 (Pb:L) complex. Although red-shifted emission band (Figure 5(b)) can be ascribed to deprotonated amide (*30*), spectroscopic studies disscused above point out the coordination of the metal cation by neutral amide in ground state. However, taking into account lower concentration range in fluorescence experiments comparing to NMR studies, deprotonation of ligand in excited state cannot be excluded under measurement conditions. Red shift of fluorescence band can also be an effect of exciplex or excimer formation in excited state.

Naphthalene derivatives **1** and **2** solutions showed incerease of fluorescence intensity in the presence of lead(II) perchlorate (Figure SM3, Supplementary Data) with good linear response: fluorecence intensity-lead(II) concentration.

For ligands **1**–**4**, changes in absorption spectra were observed also in the presence of copper(II) perchlorate in acetonitrile. Anthrylamides **3** and **4** disclose similar behaviour in Cu^{2+} binding. In absorption spectra, the two bands observed at 363 and 380 nm for free ligands disappear when copper salt is added (Figure 10). The analysis of spectrophotometric titration data reveals the formation of Cu_2L complexes in both cases. In the case of **3**, the increase in absorbance in the range of 410 to 500 nm can be explained by the formation of insoluble species during titration. Thus, given in Table 2, binding constant should be treated as an estimative value. Precipitation can be an effect of formation of insoluble species in acetonitrile copper(II)-**3** complex with perchlorate as a counterion. When copper(II) chloride was used as a salt, no precitiation was observed. However, the use of copper(II) chloride in UV–vis complexation studies is limited from analytical point of view due to overlapping of absorption bands of salt and complex (Figure SM4, Supplementary Data).

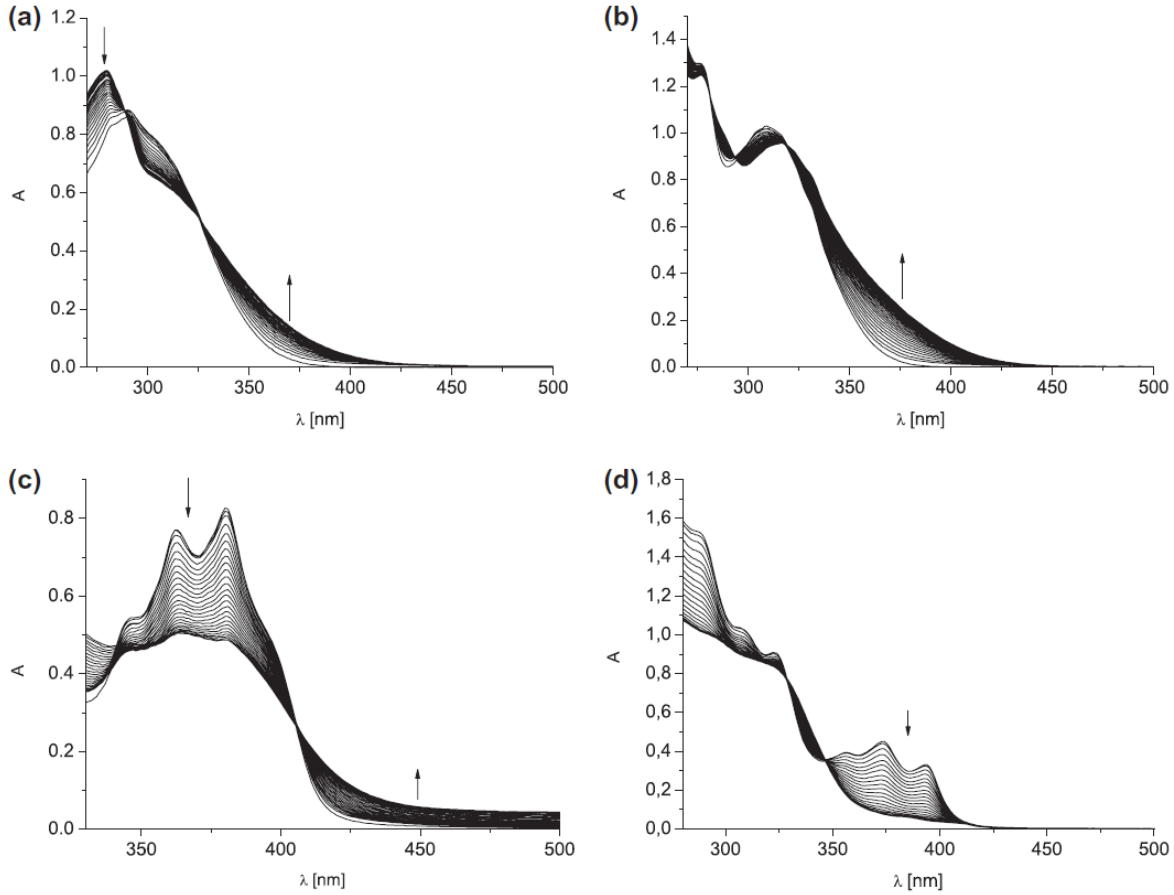

Figure 10. Changes in the UV-vis spectra upon titration with $Cu(ClO_4)_2$ (a) **1** (c_L = 5.04 × 10^{-5} M, 0 ≤ R ≤ 5.76), (b) **2** (c_L = 3.02 × 10^{-5} M, 0 ≤ R ≤ 12.4), (c) **3** (c_3 = 6.03 × 10^{-5} M, 0 ≤ R ≤ 4.80) and (d) **4** (c_L = 3.27 × 10^{-5} M, 0 ≤ R ≤ 8.69) in acetonitrile. R: salt/ligand molar ratio.

UV–vis spectra of amide derivatives **1** and **2** also undergo changes upon titration with copper(II) salt (Figure 10). It was assumed that in both cases, 1:1 complexes are formed. The value of stability constant of complex **2**–copper(II) is the lowest among all studied here complexes. The stoichiometries and obtained values of copper(II) complexes of ligands **1**–**4** in acetonitrile are collected in Table 2.

Table 2. Stoichiometries (Cu:L) and values of stability constants (log ***β***) for complexes with ligands **1-4** in acetonitrile.

Cu:L aromatic ring substitution	Ligand **1 α-**	Ligand **2 β-**	Ligand **3 α-**	Ligand **4 β-**
1:1	3.89±0.06	3.56±0.01	-	-
2:1	-	-	7.92±0.06	8.40±0.02

The reversible complexation/decomplexation of copper(II) by investigated amides is counterion dependent. In experiments where copper(II) perchlorate was used as a reversible metal cation, binding was possible to trigger by changing the pH (ethylenediamine) of solution only for naphthyl derivatives. For anthrylamides, the reversibility of complexation was observed only when copper(II) chloride was used. From UV–vis measurements, the L_D of **1** and **2** for copper cation were found to be respectively: 8.99×10^{-6}/6.83×10^{-6} M. The values 5.77×10^{-6} and 1.33×10^{-5} M obtained for **3** and **4** from titration with copper(II) perchlorate must be treated only as indicative.

FTIR spectra analysis of prepared copper(II) complexes of **3** and **4** indicates metal cation complexation through the amide oxygen atom. A comparison of FTIR spectra of 'free' ligands **3** and **4** and their copper(II) complexes is shown in Figure 11.

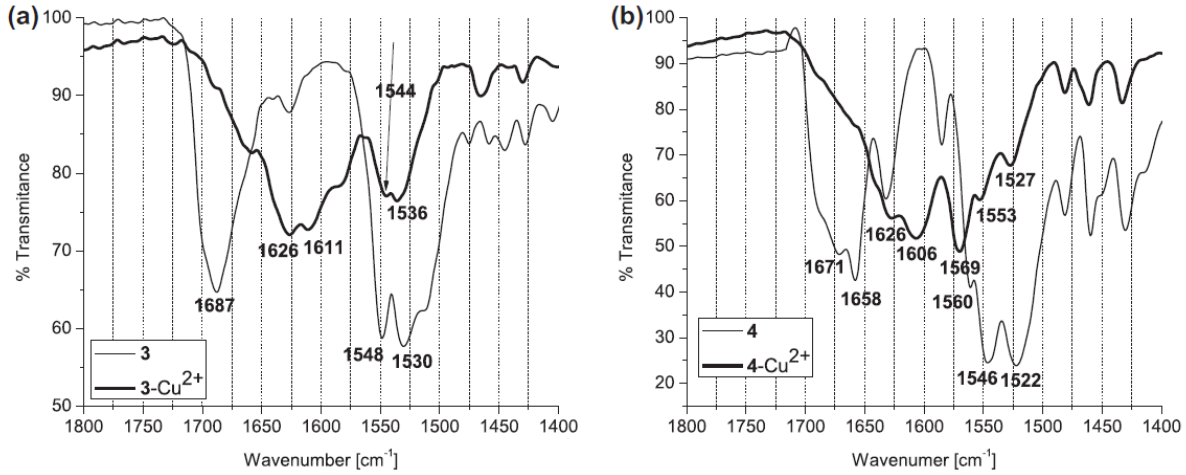

Figure 11. Comparison of normalised FTIR spectra (KBr pellet) of (a) ligand **3** and its complex with copper(II) perchlorate (1:2: w/w; **3**:copper(II) salt) and (b) ligand **4** and its complex with copper(II) perchlorate (1:2 w/w; **4**:copper(II) perchlorate).

Emission spectra of ligands **1**–**4** show fluorescence turn-off upon Cu^{2+} salt addition. In the case of naphthalene derivatives, **1** and **2** systems equilibrate within a certain time, which is about 30 min (Figure SM5, Supplementary Data). For ligands **3** and **4**, the effect of fluorescence quenching by copper(II) was different depending on the place of substitution of anthracene ring (Figure 12). In the ground state, formation of compelexes 2:1 (Cu:L) was found to be the most probable. Thus, red shift of fluorescence band of **4** – similar to the lead(II) system – contends for excimer/exciplex existance in excited state.

Copper(II) as a heavy ion is a well-known fluorescence quencher (*29*). Perchlorate, large and heavy counterion, can also contribute to fluorescence quenching process. Chlorides are weak fluorescence quenchers. In fact, the fluorescence quenching with copper(II) as a chloride salt needs higher concentration of salt given as molar ratio R (Figure SM6, Supplementary Data). For better understanding the effect of counterion in fluorescence quenching of ligands **3** and **4** by cooper(II), analogous experiments were carried out using tetra-*n*-butylammonium perchlorate and chloride. Simple comparison of Stern–Volmer constant ($\log K_{sv}$) values due to nonlinear relationship I_0/I vs. quencher concentration for copper(II) salts cannot give representative information; thus, we compared relative change of fluorescence $(I_0-I) \times 100\%$ for different salts as quenchers (Figure 13). As expected,

quenching effect of salts can be put in the following order $Cu(ClO_4)$ > $CuCl_2$ > $TBAClO_4$ > TBACl well observed for **3** having α-substituted anthracene moiety. This dependence is also obeyed to some extent for amide **4** with *β*-substituted aromatic rings; however, general effect of quenching in the last case is smaller than for ligand **3**.

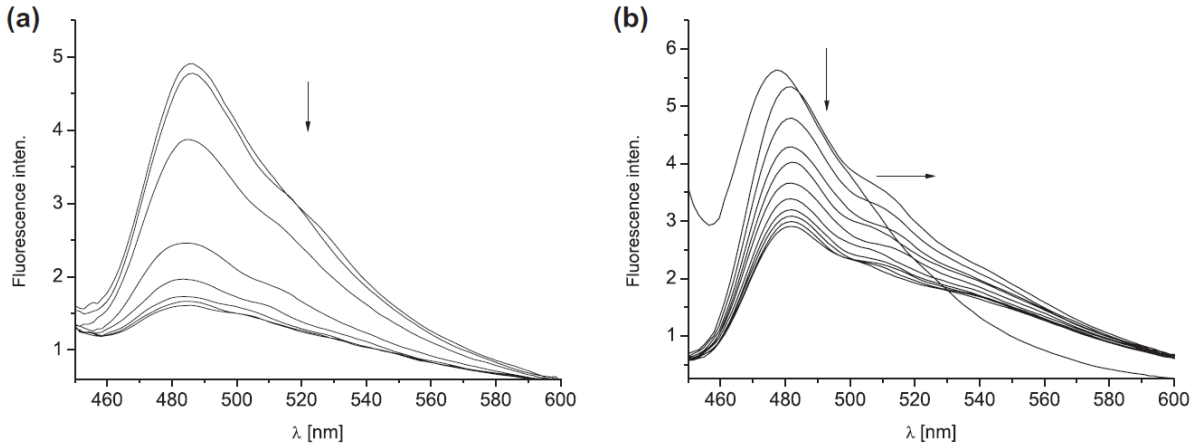

Figure 12. Changes in fluorescence spectra upon titration with $Cu(ClO_4)_2$ for ligands: (a) **3** (c_L = 3.29 × 10^{-5} M, 0 ≤ R ≤ 0.15) and (b) **4** (c_L = 4.44 × 10^{-5} M, 0 ≤ R ≤ 0.37), (λ_{ex} = 340 nm, λ_{em} = 490 nm) in acetonitrile. R: salt/ligand molar ratio.

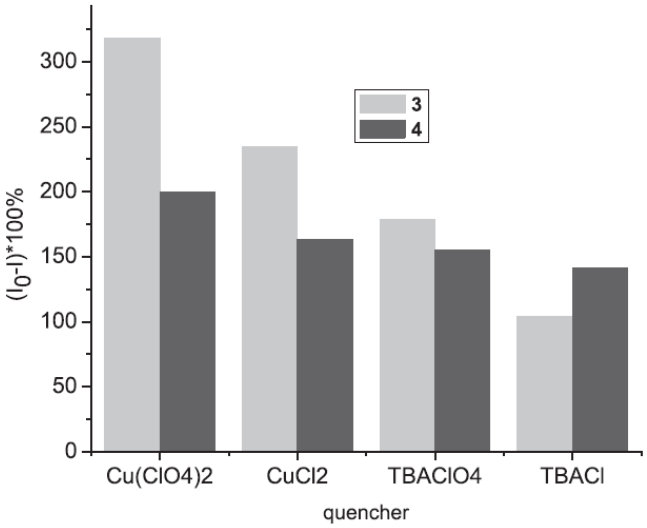

Figure 13. Fluorescence quenching of **3** and **4** by copper(II) and tetra-*n*-butylammonium salts in acetonitrile. I_0 – fluorescence of 'free' ligand, I – limiting fluorescence in the presence of quencher.

2.2.2. Competitive metal cation complexation

The influence of several potentially interfering ions on lead coordination was studied. Among tested ions were heavy metal cations: copper(II), zinc(II) and silver(I) and metal cations of high abundance in environment: sodium, potassium, magnesium and calcium. To investigate the selectivity of ligands **1**–**4** towards lead(II) cations in acetonitrile, the spectrophotometric response of ligand solution in the presence of 1 equivalent of lead(II) perchlorate before and after addition of interfering metal cation (in 10-fold molar excess) was measured. The interference from metal cations is here defined as the relative response (%RR). The results are summarised in Figure 14. In the case of all studied ligands, the most interfering ion in lead(II) coordination is copper(II) cation. Anthracene-based ligands **3** and **4** reveal better selectivity towards lead(II) cations than naphthalene-derived amides **1** and **2**. For both ligands

3 and **4**, the value of relative response for tested metal cations, except of copper(II) cations, is lower than 5%, what indicates negligible influence of those ions on interactions between anthracene-based receptors and lead(II) cations.

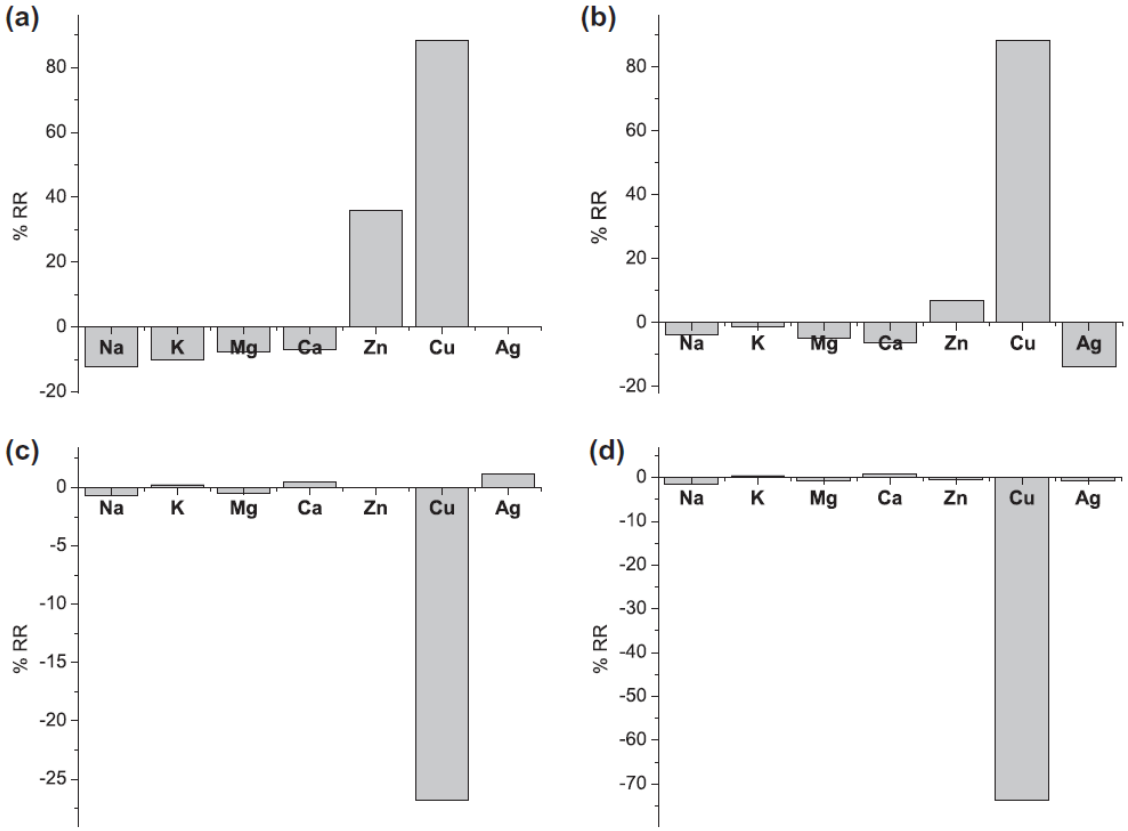

Figure 14. Interferences from several metal cation (10-fold molar excess) to the spectrophotometric determination of $Pb(ClO_4)_2$ (1 equivalent) by ligand (a) **1** (c_L = 2.95 × 10^{-5} M, λ = 370 nm), (b) **2** (c_L = 6.57 × 10^{-5} M, λ = 400 nm), (c) **3** (c_L = 4.79 × 10^{-5} M, λ = 380 nm) and (d) **4** (c_L = 2.78 × 10^{-5} M, λ = 380 nm) in acetonitrile.

3. Conclusions

Pyridine-2,6-dicarboxamides bearing aromatic condensed rings are selective receptors of biologically and environmentally important lead(II), copper(II) cations with L_D order of 10^{-6} M. In acetonitrile, ion binding and connected with it spectral response were found to be dependent both on the type of aromatic residue and steric effects of naphthalene or anthracene moiety. Newly synthesised anthracene-based diamides stronger bind investigated metal cations than their naphtalene-containing analogues. Since many pyridine-2,6-dicarboxamides are bioactive compounds, they can affect Cu concentrations, what can result in treatement of various diseases. On the other hand, presented studies of ion binding properties of investigated ligands can contribute to developpment of therapeutic systems in which complexes of bioactive ligands are used.

4. Experimental

4.1. Materials and methods

All chemicals of the highest available purity were purchased from commercial sources and used without further purification. DMF for synthesis was dried before use over A4

molecular sieves. The reaction progress was monitored by TIC using aluminium sheets covered with silica gel $60F_{254}$ purchased from Merck. ^{1}H NMR spectra were recorded on 200- or 500-MHz apparatus in DMSO-d_6 or acetone-d_6. ^{13}C NMR spectra were recorded on 125-MHz apparatus in DMSO-d_6. Chemical shifts are reported as δ [ppm] values in relation to TMS. For FT-MIR spectra, KBr pellet technique was used. High-resolution mass spectra were recorded on double-focusing magnetic sector instrument. For spectrophotometric measurements, 1-cm quartz cuvettes were used. Fluorescence spectra were recorded on luminescence spectrometer using flash xenon lamp. Bandpass of excitation and emission monochromators was 16 nm. Fluorescence spectra are uncorrected to instrument response. All emission spectra were recorded three times and averaged. UV–vis and fluorescence measurements were carried out using acetonitrile (LiChrosolv®) of gradient grade. All salts, purchased from commercial resources, used in spectroscopic measurements, were dried under vacuum at room temperature before use. Stock solutions of metal salts were standardised by complexometric titration with EDTA (*31*).

4.2. Synthesis

Diamides **1–4** were prepared using simple synthetic method (*22, 23*) where pyridine-2,6-dicarboxylic acid chloride (1 mmol) was added stepwise to the solution of the respective amine (2 mmol) and triethylamine (2 mmol) in DMF (15 ml). The reaction mixture was magnetically stirred at 60°C for 12 h. To the cooled reagents, water was added and precipitate was filtrated off. Pure product was obtained after crystallisation from propan-2-ol.

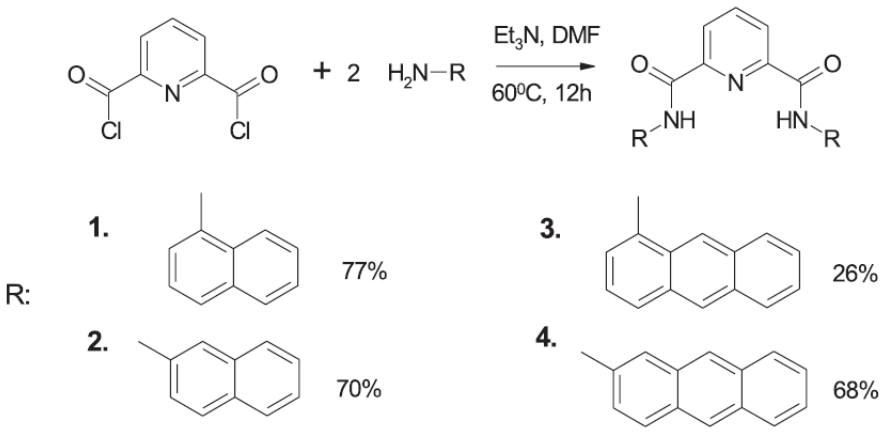

Scheme 1. Synthetic route for ligands **1**-**4**.

***N,N′*-bis(1-naphthyl)pyridine-2,6-dicarboxamide (1):** 32 mg, 77% (lit. 81% (*18*) and 55% (*23*)); white solid; mp 231°C; R_f = 0.80 (dichloromethane: methanol, 15:2, v/v); ^{1}H NMR (200 MHz, DMSO-d_6): δ = 7.28 (1H, s); 7.32 (2H, t, J = 9.0 Hz); 7.48 (2H, t, J = 8.5 Hz); 7.72 (2H, d, J = 11.0 Hz); 7.9 (2H, d, J = 7.6 Hz); 8.45 (2H, t, J = 9.4 Hz); 8.16 (2H, d, J = 7.4 Hz); 8.29 (2H, d, J = 8.5 Hz); 8.53 (2H, d, J = 7.8 Hz); 10.26 (2H, s); FT-MIR (KBr pellet): 3299; 3050; 1675; 1660; 1544; 1502; 1349; 791; 770; 652 cm^{-1}; UV–vis (acetonitrile): $\lambda(\varepsilon)$ = 290 (1.7 × 10^4); fluorescence: λ_{ex} = 240 nm, λ_{em} = 350 nm.

***N,N′*-bis(2-naphthyl)pyridine-2,6-dicarboxamide (2)**: 29 mg, 70%; white solid mp 260°C; R_f = 0.80 (dichloromethane: methanol, 15:2, v/v); ^{1}H NMR (500 MHz, DMSO-d_6,): δ = 7.48 (4H, t, J = 9.9 Hz); 7.92 (4H, d, J = 5.9 Hz); 7.98 (2H, s); 8.10 (2H, s); 8.32 (1H, t, J = 7.6 Hz); 8.46 (2H, d, J = 5.2 Hz); 8.60 (2H, s); 11.20 (2H, s); FT-MIR (KBr pellet): 3283; 3057; 1671; 1659; 1547; 1505; 1363; 814; 748; 682 cm^{-1}; UV–vis (acetonitrile): $\lambda(\varepsilon)$ = 311 nm (3.4 × 10^4); fluorescence: λ_{ex} = 230 nm, λ_{em} = 350 nm; HRMS (EI) m/z: $[M]^+$ Calculated for $C_{27}H_{19}N_3O_2$ 417.14773; Found 417.14653.

***N,N′*-bis(1-anthryl)pyridine-2,6-dicarboxamide (3):** 13 mg, 26%, golden-green solid; mp 260°C; R_f = 0.86 (dichloromethane: methanol, 15:2, v/v); ^{1}H NMR (500 MHz, DMSO-d_6): δ

= 7.39 (2H, t, *J* = 7.5 Hz); 7.49 (2H, t, *J* = 7.5 Hz); 7.58 (2H, t, *J* = 7.8 Hz); 7.71 (2H, d, *J* = 7.0 Hz); 8.06 (4H, d, *J* = 8.5 Hz); 8.18 (2H, d, *J* = 8.5 Hz); 8.39 (1H, t, *J* = 7.8 Hz); 8.65 (2H, s); 8.84 (2H, s); 11.60 (2H, s); ^{13}C NMR (125 MHz, DMSO-d_6, 50 °C): δ = 122.74; 124.10; 125.69; 126.04; 126.41; 126.58; 127.26; 127.70; 128.49; 128.66; 129.27; 131.85; 131.97; 132.56; 133.92; 140.75; 149.80; 163.61; FT-MIR (KBr pellet): 3265; 3032; 1672; 1641; 1524; 1430; 781; 653 cm^{-1}; UV–vis (acetonitrile): $\lambda(\varepsilon)$ = 362 nm (1.3 × 10^4), 380 nm (1.4 × 10^4); fluorescence: λ_{ex} = 340 nm, λ_{em} = 490 nm; HRMS (EI) m/z: [M]$_+$ Calculated for $C_{35}H_{23}N_3O_2$ 517.1790; Found 517.1788.

***N,N′*-bis(2-anthryl)pyridine-2,6-dicarboxamide (4):** 35 mg, 68%, green solid; mp 274°C; R_f = 0.86 (dichloromethane: methanol, 15:2, v/v); ^{1}H NMR (500 MHz, DMSO-d_6): δ = 7.52 (4H, q, *J* = 6.4 Hz); 8.06 (2H, d, *J* = 9.3 Hz); 8.11 (4H, d, *J* = 8.3 Hz); 8.23 (2H, d, *J* = 9.3 Hz); 8.40 (1H, t, *J* = 7.8 Hz); 8.52 (2H, d, *J* = 7.8 Hz); 8.61 (4H, d, *J* = 4.4 Hz); 8.84 (2H, s); 11.36 (2H, s); ^{13}C NMR (125 MHz, DMSO-d_6, 50 °C): δ = 116.45; 122.10; 125.04; 125.28; 125.55; 125.80; 127.63; 127.92; 128.62; 128.83; 130.67; 131.31; 131.63; 135.02; 139.89; 148.82; 161.90; FT-IR (KBr pellet): 3274; 3048; 1672; 1658; 1546; 1524; 1459; 886; 741; 684; 647 cm^{-1}; UV–vis (acetonitrile): $\lambda(\varepsilon)$ = 357; 373; 393 nm (1.2 × 10^4; 1.4 × 10^4; 1.0 × 10^4); fluorescence: λ_{ex} = 420 nm, λ_{em} = 480 nm; HRMS (EI) m/z: [M]$^+$ Calculated for $C_{35}H_{23}N_3O$ 517.17903; Found 517.17903.

4.3. Complexation studies

Binding properties of obtained compounds were tested using UV–vis spectrophotometry, spectrofluorimetry, ^{1}H NMR and FT-MIR spectroscopy. Spectroscopic response towards many metal cations, such as alkali, alkaline earth, heavy divalent metal cations (in the form of perchlorate salts, *caution!*) as well as anions of different size and shape (as tetra-*n*-butylammonium (TBA) salts), was investigated. UV–vis measurements were carried out at 25.0±0.1°C and at ionic strength I = 10^{-2} M using tetraethylammonium perchlorate (Et_4NClO_4) as a supporting electrolyte and acetonitrile as a solvent. The spectral changes of ligand solution of defined concentration (2.5 ml) were recorded upon stepwise addition of 10 µl of the salt solution (titration step) directly into the measurement cell. On the basis of experimental data, the stability constant values and stoichiometry of species were determined using the SPECFIT software (*32*). The L_D were calculated from plots A = f (concentration of metal perchlorate) using equation:

$$L_D = \frac{3\sigma}{K}$$

where σ is the standard deviation of the bank and K is the slope of the linear calibration range.

4.4. Complexes preparation and characterization

For ^{1}H NMR and FTIR studies, complexes of ligands with salts were prepared by dissolving equimolar (8 mmol) amounts of respective ligand and lead(II) perchlorate in acetone (10 ml). For copper(II) complex preparation, twofold molar excess of salt was used. The respective mixture was refluxed till homogenous solution was obtained. Samples were analysed, after solvent evaporation under reduced pressure, without further purification. For **4**-Pb system, additional sample was prepared: with two-fold excess of lead(II) perchlorate. Spectra of complexes were registered in acetone-d_6 due to its similarity to acetonitrile-d_3 and wider accessibility of this popular solvent. ^{1}H NMR (500 MHz) data for spectra of ligands and their complexes registered in acetone-d_6 are given below:

3: ^{1}H NMR: δ = 7.24 (2H, t, *J* = 7.4 Hz); 7.44 (2H, t, *J* = 7.1 Hz); 7.59 (2H, t, *J* = 7.7 Hz); 7.94 (2H, d, *J* = 8.5 Hz); 7.99 (2H, d, *J* = 7.1 Hz); 8.03–8.06 (4H, m); 8.48 (1H, t, *J* = 7.7 Hz); 8.60 (2H, s); 8.65 (2H, d, *J* = 7.7 Hz); 8.95 (2H, s); 11.15 (2H, s).

3-Pb: ^{1}H NMR: δ = 7.51 (2H, t, *J* = 7.9 Hz); 7.57 (2H, t, *J* = 7.9 Hz); 7.65 (2H, t, *J* = 8.5 Hz); 7.84 (2H, d, *J* = 7.3 Hz);

8.12–8.19 (4H, m); 8.22 (2H, d, *J* = 8.5 Hz); 8.71 (2H, s); 8.89 (2H, s); 8.96 (1H, t, *J* = 7.3 Hz); 9.24 (2H, d, *J* = 7.3 Hz); 11.50 (2H, s).

4: ^{1}H NMR: δ = 7.48–7.57 (4H, m); 8.05–8.14 (6H, m); 8.19 (2H, d, *J* = 9.1 Hz); 8.42 (1H, t, *J* = 7.4 Hz); 8.56–8.62 (6H, m); 8.94 (2H, s); 10.10 (2H, s).

4-Pb ^{1}H NMR: δ = 7.52–7.58 (4H, m); 7.99 (2H, dd, J1 = 1.8 Hz; J2 = 7.3 Hz); 8.09–8.14 (4H, m); 8.21 (2H, d, *J* = 9.3 Hz); 8.58 (2H, s); 8.61(2H, s); 8.77–8.23 (3H, m); 9.03 (2H, d, *J* = 7.9 Hz); 11.14 (2H, s).

4-Pb (excess of lead(II) perchlorate) ^{1}H NMR: δ = 7.52– 7.58 (4H, m); 8.00 (2H, dd, J1 = 1.8 Hz; J2 = 9.1 Hz); 8.09–8.14 (4H, m); 8.22 (2H, d, *J* = 9.1 Hz); 8.60 (2H, s); 8.62(2H, s); 8.81–8.88 (3H, m); 9.14 (2H, d, *J* = 7.9 Hz); 11.18 (2H, s).

4.5. Competitive complexation experiments

In competition studies, the absorbance of ligand solution in the presence of lead(II) perchlorate at fixed concentration (1 equivalent) was recorded before (A_0) and after (A) addition of interfering metal cations (as perchlorate salts) at the concentration 10 times higher than the analyte. The influence of tested interfering ions on spectrophotometric determination of lead(II) cations is presented as the relative response. The value of the relative response was determined as $\%RR = [(A-A_0)/A_0]\times 100\%$.

Disclosure statement

No potential conflict of interest was reported by the authors.

Funding

This work was supportted by the Development of Interdisciplinary Doctoral Studies at the Gdansk University of Technology in Modern Technologies, project no: POKl.04.01.01-00-368/09, and [grant number 030363T001] Gdansk University of Technology. E.W.-W. Kindly acknowledged support from sources for science in years 2010–2011, [grant number N N204 137438].

References

(1) Atwood, J.L.; Davies, J.E.D.; Macnicol, D.D.; Vögtle, F., Eds.; *Comprehensive Supramolecular Chemistry*; Pergamon Press: New York, NY, 1996; Cragg, P.J. *Supramolecular Chemistry. From Biological Inspiration to Biomedical Applications*; Springer Science+Business Media B.V: Dordrecht, 2010; Steed, J.W.; Gale, P.A. *Supramolecular Chemistry; From Molecules to Nanomaterials*; Wiley: Chichester, UK, 2012.

(2) Gillis, B.S.; Arbieva, Z.; Gavin, I.M. *BMC Genomics*. 2012, *13,* 344 and references cited therein.

(3) Nordberg, G. *Handbook on the Toxicology of Metals*; Academic Press: New York, 2007; pp 529–600.

(4) Martínez-Máñez, R.; Sancenon, F. *Chem. Rev.* 2003, *103,* 4419–4476.

(5) Veale, E.B.; Gunnlaugsson, T. *Annu. Rep. Prog. Chem. Sect. B*. 2010, *106,* 376–406.

(6) Miyaji, H.; Anzenbacher, P., Jr.; Sessler, J.L.; Bleasdale, E.R.; Gale, P.A. *Chem. Commun.* 1999, 1723–1724.

(7) Quinn, W.A.; Saeed, M.A.; Powell, D.R.; Hossain, Md.A. *J. Environ. Res. Public Health* 2010, *7,* 2057–2070.

(8) Watt, M.M.; Collins, M.S.; Johnson, D.W. *Acc. Chem. Res.* 2013, *46,* 955–966.
(9) Patra, A.K., Mukherjee, R. *Inorg. Chem.* 1999, *38,* 1388–1389 and references therein.
(10) Renaud, F.; Piguet, C.; Bernardinelli, G.; Bünzli, J.-C.G., Hopfgartner, G. *Chem. Eur. J.* 1997, *3,* 1646–1659.
(11) Picot, A.; Malvolti, F.; Guennic, B.L.; Baldeck, P.L.; Williams, J.A.G.; Andraud, C.; Maury, O. *Inorg. Chem.* 2007, *46,* 2659–2665.
(12) Huang, D.; Makhlynets, O.V.; Tan, L.L.; Lee, S.C.; Rybak-Akimova, E.V.; Holm, R.H. *Inorg. Chem.* 2011, *50,* 10070–10081.
(13) Leung, W.-H.; Ma, J.-X.; Yam, V.W.-W.; Che, C.-M.; Poon, C.-K. *J. Chem. Soc.*, Dalton Trans., 1991, *4,* 1071–1076.
(14) Amini, M.; Navidpour, L.; Shafiee, A. *DARU* 2008, *16,* 9–12. Al-Salahi, R.A.; Al-Omar, M.A.; Amr, A.E. *Mol.* 2010, *15,* 6588–6597; Özdemir, N.; Dayan, O.; Çetinkaya, B.; Akgül, C. *Spectrochim. Acta A Mol. Biomol. Spectrosc.* 2012, *86,* 614–624.
(15) Granotier, C.; Pennarun, G.; Riou, L.; Hoffschir, F.; Gauthier, L.R.; De Cian, A.; Gomez, D.; Mandine, E.; Riou, J.-F.; Mergny, J.-L.; Mailliet, P.; Dutrillaux, B.; Boussin, F.D. *Nucleic Acid Res.* 2005, *33,* 4182–4190.
(16) Crans, D.C. *Inorg. Biochem.* 2000, *80,* 123–131; Crans, D.C.; Yang, L.; Alfano, J.A.; Chi, L.-H.; Jin, W.; Mahroof-Tahir, M.; Robbins, K.; Toloue, M.M.; Chan, L.K.; Plante, A.J.; Grayson, R.Z.; Willsky, G.R. *Coord. Chem. Rev.* 2003, *237,* 13–22.
(17) Lebon, F.; Iedecq, M.; Dieu, M.; Demazy, C.; Remacle, J.; Lapouyade, R.; Kahn, O.; Durant, F. *J. Inorg. Chem.* 2001, *86,* 547–554.
(18) Hiratani, K.; Taguchi, K. *Bull. Chem. Soc. Jpn.* 1990, *63,* 3331–3333.
(19) Ghosh, K.; Kumar, S.; Kumar, R.; Singh, U.P. *J. Organomet. Chem.* 2014, *750,* 169–175.
(20) Qi, J.; Zhou, Z.; Chan, A.S.C. *Acta Crys.* 2001, *57,* 749–750.
(21) Sigel, H.; Martin, R.B. *Chem. Rev.* 1982, *82,* 385–462.
(22) Wagner-Wysiecka, E.; Chojnacki, J. *Supramol. Chem.* 2012, *24,* 684–695.
(23) Wagner-Wysiecka, E.; Łukasik, N. *Tetrahedron Lett.* 2012, *53,* 6029–6034.
(24) Łukasik, N.; Wagner-Wysiecka, E.; Hubscher-Bruder, V.; Michel, S.; Bocheńska, M. *Logistyka* 2014, *4,* 318–324.
(25) Kim, J.; Morozumi, T.; Hiraga, H.; Nakamura, H. *Anal. Sci.* 2009, *25,* 1319–1325; Kim, J.; Oka, Y.; Morozumi, T.; Choi, E.W.; Nakamura, H. *Tetrahedron* 2011, *67,* 4814–4819.
(26) Younes, A.H.; Clark, R.J.; Zhu, L. *Supramol. Chem.* 2012, *24,* 696–706; Lee, D.N.; Ryu, J.Y.; Kwak, H.; Lee, Y.M.; Lee, S.H.; Poong, J.I.; Lee, J.; Shin, W.; Kim, C.; Kim, S.-J.; Kim, Y. *J. Mol. Struct.* 2008, *885,* 56–63; Briand, G.G.; Smith, A.D.; Schattte, G.; Rossini, A.J.; Schurko, R.W. *Inorg. Chem.* 2007, *46,* 8625–8637; Norkus, E.; Gaidamauskas, E.; Stalnioniene, I.; Crans, D.C. *Heteroat. Chem.* 2005, *16,* 285–291; Brandi-Blanco, M.P.; Choquesillo-Lazarte, D.; García-Collado, C.G.; González-Pérez, J.M.; Castiñeiras, A.; Niclos-Gitiérrez, J. *Inorg. Chem. Commun.* 2005, *8,* 231–234.
(27) Zafiropoulos, T.F.; Perlepes, S.P.; Ioannou, P.V.; Tsangaris, J.M.; Galinos, A.G.Z. *Naturforsch. B* 1981, *36,* 87–93; Nelwamondo, A.N.; Eve, D.J.; Watkins, G.M.; Brown, M.E. *Termochim. Acta* 1998, *318,* 165–175; Reddy, P.M.; Reddy, M.B.; Rohini, R.; Shanker, K.; Ravinder, V. *Arch. Appl. Sci. Res.* 2009, *1,* 12–17; Huczyński, A.; Janczak, J.; Brzeziński, B. *Polyhedron* 2011, *30,* 2870–2877.
(28) Chmielewski, M.J.; Jurczak, J. *Tetrahedron Lett.* 2005, *46,* 3085–3088.
(29) Lakowicz, J.R. *Principles of Fluorescence Spectroscopy*, 3rd ed.; Springer Science+Business Media: New york, 2006.
(30) Galinos, A.G.; Perlepes, S.P.; Zafiropoulos, T.F.; Ioannou, P.V.; Kouinis, J.K. *Monatsh. Chem.* 1981, *112,* 1113–1121; Chavez, F.A.; Olmstead, M.M.; Mascharak, P.K. *Inorg. Chim. Acta* 1998, *269,* 269–273; Xu, Z.; Qian, X.; Cui, J.; Zhang, R. *Tetrahedron* 2006, *62,* 10117–10122; Shi, D.; Zhou, X.; Zheng, T.; Zou, Y.; Guo, S.; Lv, J.; Yan, F. *J. Iran. Chem.*

Soc. 2015, *12,* 293–308; Tian, X.; Guo, X.; Jia, L.; Yang, R.; Cao, G.; Liu, Ch *Sensor Actuat. B-Chem.* 2015, *221,* 923–929.
(31) *Methodes d'analyses complexométriques par les Titriplex*, 3rd ed.; E. Merck AG: Darmstadt, 1992, *37*; pp 51.
(32) Gampp, H.; Maeder, M.; Meyer, C.J.; Zuberbühler, A.D. *Talanta* 1985, *32,* 95–101.